

Silicon Detectors for the Super LHC

Sally Seidel, for the RD50 Collaboration

Department of Physics and Astronomy, 800 Yale Blvd. NE, MSC07 4220 University of New Mexico, Albuquerque, NM 87108 USA

Abstract

The luminosity upgrade of the Large Hadron Collider (LHC) at CERN to the Super LHC (sLHC) will increase the radiation dose at the experiments by roughly an order of magnitude. The elevated radiation levels require the LHC experiments to upgrade their tracking systems with extremely radiation hard detectors, capable of withstanding about a 1-MeV neutron-equivalent (n_{eq}) fluence of 10^{16} per square centimeter for the innermost tracking layers. Recent results on radiation hardening technologies developed by the RD50 Collaboration for sLHC use are reported. Silicon detectors have been designed and produced on n - and p -type wafers made by float zone, epitaxial and Czochralski technologies. Their charge collection efficiency after proton, neutron, pion, and mixed irradiation to sLHC fluences has been studied. Novel detector concepts have been designed, produced, and tested as well. Radiation-induced microscopic defects have been investigated and can be partly linked to the performance degradation of irradiated detectors.

Key words: Radiation damage, Silicon detectors, Large Hadron Collider, sLHC

1. Introduction

The CERN-based RD50 Collaboration, whose purpose is the development of radiation hard semiconductor devices for high luminosity colliders, has produced a broad spectrum of results this year in the areas of defect characterization and engineering and characterization and comparison of substrates in p - and n -type silicon fabricated with the epitaxial and magnetic Czochralski processes as well as float zone. Progress has continued in optimization of patterning as well as in the development of alternatives to the planar geometry known as 3D and Independent Coaxial Detector Array. The work is motivated by evidence that float zone planar n -type silicon sensors will not operate effectively in the SuperLHC environment, where the hadron fluence at radius 4 cm is expected to be about $1.6 \times 10^{16} \text{ cm}^{-2} n_{eq}$ and charge trapping is anticipated to be the primary limitation. Additional information on all of the results presented here can be found at <http://rd50.web.cern.ch/rd50/> under links to the 14th and 15th Workshops.

2. Defect Characterization and Engineering

Five studies of defect characteristics are reported. The first [1] uses high resolution photo-induced transient spectroscopy to compare radiation defects in silicon with oxygen concentrations of 4.5 and $14.0 \times 10^{16} \text{ cm}^{-3}$. The work compares trap parameters and trap concentration to oxygenation level, annealing time and temperature, and fluence. The investigators find that high oxygen concentration mainly affects shallow traps related to interstitial aggregates; mid-gap traps develop independently of oxygen concentration after annealing at 240°C , and the number of traps is maximized in both the standard and the more highly oxygenated epitaxial layers after

annealing at 80° and 160°C . The study examines the evolution of trap concentrations with fluence, concluding for example that the dominant trap in low-fluence epitaxial n -type material with standard oxygenation lies at 410 meV and is likely to be I_2O . As the fluence rises, the 315 meV trap, likely V_xO_y , comes to dominate. In oxygenated ($[O] = 14.0 \times 10^{16} \text{ cm}^{-3}$) n -type epitaxial silicon, the 420 meV (likely $V_2^{-/0}$) trap dominates at all fluences ($\leq 1.7 \times 10^{16} \text{ p cm}^{-2}$) examined, while after 1 hour of 240°C annealing, the dominant defect is at 575 meV.

A DLTS study [2] of p -type silicon irradiated with 6 MeV electrons and alphas finds that self-interstitial silicon can persist after irradiation at 273 K when the ratio of electron-hole generation rate to Frenkel pair generation rate is small. Injection of current at liquid nitrogen temperature removes this defect.

A study [3] has been made of the shallow donor E(30K) generated by electron irradiation of n -type float zone silicon diodes. E(30K), a cluster defect associated with non-type inversion of epitaxial diodes after high proton fluence, overcompensates deep acceptors. In this study the generation rate was found to be suppressed for high electron energies, leading to speculation about the possibility of a point-like characteristic.

A TSC study [4] of p - and n -type magnetic Czochralski silicon irradiated with reactor neutrons up to $10^{16} \text{ cm}^{-2} n_{eq}$ observes features thought to be due to a residual electric field, a polarization of the irradiated silicon bulk opposed to the external bias, which arises as a result of charged traps frozen in the bulk and barriers close to the electrodes.

3. Epitaxial Silicon

Epitaxial silicon has been examined as a promising substrate both for the enhanced oxygenation intrinsic to the process and for the opportunity to obtain well-controlled thin layer growth.

TCT studies and a simulation of charge collection in $150\mu\text{m}$ thick epitaxial devices after fluences in the range 1 to $4 \times 10^{15} \text{ cm}^{-2} n_{\text{eq}}$ have revealed [5] an electric field (E)-dependent contribution to carrier lifetimes. The charge collection and trapping are well described by $-dN = \frac{1}{\tau(E(x(t)))} N dt$, for $\tau = \tau_0 + \tau_1 E$, in a model that includes distortions to the space charge distribution leading to parabolic electric fields (i.e., a double peak) and electronic circuit effects in TCT signals. The trapping probability decreases with increasing electric field, suggesting that well controlled high fields are desirable to reduce trapping.

Studies [6] of charge multiplication in highly irradiated sensors were reported. Devices fabricated on n -type epitaxial silicon with $[O] = 9 \times 10^{16} \text{ cm}^{-3}$, orientation $\langle 111 \rangle$, and $N_{\text{eff},0} = 2.6 \times 10^{13} \text{ cm}^{-3}$, when irradiated with 10^{16} cm^{-2} 24-GeV protons, respond with a signal showing proportional response, long-term stability, and homogeneous production, with only slight noise increase relative to the unirradiated state. A two-parameter theoretical model [7] of this has been constructed assuming avalanche multiplication in $p-n$ junctions and an E field controlled by current injection in deep-level doped semiconductors. It uses the electric field in the detector base region and potential sharing between the base and the depleted region adjacent to the segmented side. It predicts that charge multiplication can only occur in detectors with segmented $n+$ sides.

4. Czochralski Silicon

Preparation of the ingot through the magnetic Czochralski (MCz) process automatically enhances the oxygen content of the substrate, providing resistance to radiation damage by charged hadrons. A recent study [8] comparing depletion voltage and leakage current of n -type float zone (FZ) and n -type MCz silicon after irradiation by 24 GeV protons or 300 MeV pions has reached the preliminary conclusion that the MCz collects more charge than the FZ after equivalent fluence and that the collected charge with either substrate is less after pion irradiation than after protons.

A four-trap level device model [9] has been developed for neutron damage effects in n -type MCz material. The model produces good agreement on full depletion voltage and leakage current between simulation (based on Synopsis TCAD) and data, for fluences from about 0.5 to $3.0 \times 10^{14} \text{ cm}^{-2} n_{\text{eq}}$. Associated theoretical calculations based on Shockley Read Hall recombination theory reproduce the full depletion voltage data but underestimate the measured leakage current at 293 K. An enhancement of the model to describe charge carrier trapping and the electric field distribution following a mixed irradiation is under development.

A study [10] of low resistivity n -type MCz material has been undertaken, motivated by known challenges to maintaining electrical isolation of channels in p -type material. A comparison with new and previously reported measurements on p - and n -type float zone and MCz substrates shows charge collection efficiency competitive with p -type float zone devices after fluences of a few times $10^{15} \text{ cm}^{-2} n_{\text{eq}}$. The challenge for operation in this mode continues to be associated high current.

A mixed irradiation of MCz sensors has been undertaken, maintaining a ratio of charged to neutral hadrons consistent with what is expected at the sLHC over tracker radii from 0 to 150 cm . Trapping times in MCz silicon have been extracted [11] for fluences up to $10^{15} \text{ cm}^{-2} n_{\text{eq}}$.

5. Comparisons of p - and n -type Silicon

The benefits of sensors based on p -type silicon include the absence of radiation-induced type inversion, the cost reduction associated with single-sided processing, and the collection of electrons.

An Edge-TCT study [12] of long term annealing on p -type float zone sensors irradiated to $5 \times 10^{15} \text{ n/cm}^2$ shows an increase in charge collection by a factor of approximately 2.8 as the annealing time at 60° C is increased from 80 to 10240 minutes.

A study [13] of charge collection in n -in- p planar sensors after neutron, proton, and pion irradiation shows, after correction for annealing in the pion and proton samples, that the charge collected by float zone devices may still be competitive at the innermost layer of an sLHC detector up to fluences as high as $2 \times 10^{16} \text{ cm}^{-2} n_{\text{eq}}$. Figure 1 shows the collected charge as a function of fluence.

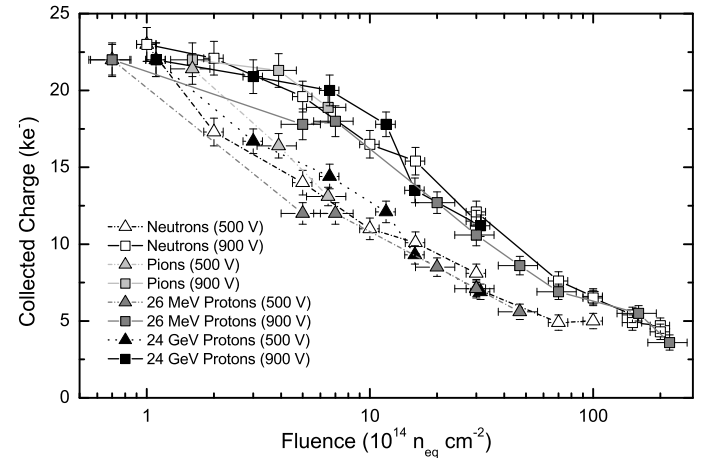


Figure 1: Collected charge at biases of 500 V and 900 V as a function of fluence for n -in- p FZ sensors irradiated with neutrons, 280 MeV pions, 26 MeV protons, and 24 GeV protons up to $2.2 \times 10^{16} \text{ cm}^{-2} n_{\text{eq}}$. The pion and 24 GeV proton data are corrected for the annealing that occurred during the irradiation [13].

A study [14] of full depletion voltage after high irradiation by 800 MeV protons followed by a 60° C anneal has been conducted for p -type and n -type float zone and MCz devices. Beneficial annealing is observed for the first 80 minutes, after which the full depletion voltage begins to increase for samples shown to have negative space charge, i.e., all but the p -on- n MCz device. Beyond $10^{14} \text{ cm}^{-2} n_{\text{eq}}$, the float zone devices show the greatest increase in full depletion voltage with fluence, while the n -on- p MCz shows little change up to $10^{16} \text{ cm}^{-2} n_{\text{eq}}$.

Charge collection efficiency of p -in- n sensors as a function of annealing time has been examined [15] for float zone devices irradiated to $2 \times 10^{14} \text{ n}_{\text{eq}} \text{ cm}^{-2}$. The annealing times examined span the range from a few times 10^3 to a few times 10^6

minutes. The study is motivated by a desire to reduce dependence upon model-based extrapolations and to compare signal to predictions in a regime where CV-based models predict under-depletion. For a device operated at bias 600 V, over a range in which the Hamburg model [16] and the model used to generate predictions in the ATLAS Tracker Technical Design Report [17] both predict under-depletion, the signal is found to remain sizeable and to diminish only slowly with growing annealing time.

6. Pattern Optimization

Several geometrical optimization studies are underway. In one, Synopsis Sentaurus is used to predict [18] the electric field profile and breakdown voltage for various guard ring configurations that sample the parameter space in implant, metal, and passivation geometries for fixed oxide concentrations. Up to oxide concentration 10^{12} cm^{-2} , a result has been achieved that predicts stable operation up to 900 V bias in a device exposed to fluence $10^{15} \text{ cm}^{-2} n_{\text{eq}}$.

The Lorentz angle in silicon strip sensors irradiated with 23 MeV protons has been studied [19] in a magnetic field up to 8 T. The sensor sample includes MCz and float zone silicon of both *p*- and *n*-type bulk. Lasers with wavelengths red and infrared are used for the study; the highly irradiated samples can only be measured by the infrared. The Lorentz shift increases with fluence for holes and decreases with fluence for electrons.

7. Alternatives to Planar Geometry

A simulation of the separate contributions of electrons and holes to the total charge collection by an irradiated silicon sensor has been undertaken [20]. For charge collection pitches greater than $60 \mu\text{m}$, the hole contribution is about 43% at fluence $10^{16} \text{ cm}^{-2} n_{\text{eq}}$, due to the fact that the pitch is much larger than the charge collection and trapping distances. For pitches smaller than about $60 \mu\text{m}$, the hole contribution decreases correspondingly. The hole contribution to the total collected charge increases with fluence in an *n+* segmented sensor and is, at fluence $1 \times 10^{16} \text{ cm}^{-2} n_{\text{eq}}$, comparable to that of electrons. At sLHC fluences, the total collected charge is approximately given by the formula $Q = 80e/\mu\text{m} \cdot (d_{\text{CCE}}^e + d_{\text{CCE}}^h)$. To improve the radiation hardness of the device, the carrier trapping distance must accordingly be increased, for example by pre-filling of the traps or by decreasing the carrier drift distance.

Several geometries that achieve the drift distance reduction are under study by RD50 members. One, 3D, decouples thickness from charge collection distance through a geometry in which implant columns are oriented perpendicular to the planar surface. Devices by FBK-irst (Trento) and CNM (Barcelona) are being compared in two slightly different versions. The former involve empty columns (passivated with silicon oxide only), ohmic columns connected by a uniform doping layer and metalization, and AC and DC coupled readout pads [21]. The latter include columns partially filled with polysilicon, ohmic columns connected by polysilicon and metalization, and DC

coupled readout pads [22]. Tests of the FBK-irst ATLAS pixel prototypes [23, 24, 25] compare geometries in which a pixel includes 2, 3, or 4 junction columns—so-called 2E, 3E, and 4E patterns. Both CNM and FBK devices are produced with a “double-sided” architecture, in which one set of columns is etched from the front side and the other set is etched from the back side into the wafer. Dedicated reports on measurements of each of these geometries, including test beam results [26, 27] and charge collection studies of irradiated detectors [28], are included in the conference proceedings.

Simulation studies have been performed [18] on CMS-design 3D sensors manufactured by SINTEF. The studies suggest that the columns will become dead regions at fluences higher than $10^{14} \text{ cm}^{-2} n_{\text{eq}}$ and, following fluence $10^{16} \text{ cm}^{-2} n_{\text{eq}}$, that the charge collection efficiency is highest (approximately $9 ke^-$) between electrodes and lowest (approximately $5.5 ke^-$) near cell edges. A comparison of the expected performance of the 2E and 4E geometries finds, for the 2E, a lower capacitance between readout electrodes (about 0.7 fF at zero fluence for $Q_{\text{ox}} = 4 \times 10^{11} \text{ cm}^{-2}$) and less dead volume (approximately 4% of the total). For the 4E geometry, the study reports relatively faster charge collection, less trapping at high fluences, lower depletion voltage, higher breakdown voltage, larger capacitance between readout electrodes (about 3.2 fF at zero fluence for $Q_{\text{ox}} = 4 \times 10^{11} \text{ cm}^{-2}$), and larger dead volume (approximately 8% of the total).

A new electrode geometry, using novel asymmetric electrode configurations to produce homogeneous well-defined electric fields throughout the sensor, has been presented [29]. This Independent Coaxial Detector Array pattern has been implemented in two different designs, the “concentric type,” which produces an electric field with nearly zero θ dependence, and the “parallel plate type,” which produces a near linear electric field. The predicted total collected charge is 39%, and the dead space can be reduced below 14% for a sLHC implementation.

8. Summary

Major advances have been made in correlation of microscopic defect properties with observed material characteristics. New information is available on epitaxial, Czochralski, and *p*-bulk silicon substrate properties. Work is ongoing to understand and optimize Lorentz angle, guard rings, and other design features. New geometries including 3D and Independent Coaxial Detector Array continue to evolve.

References

- [1] P. Kaminski, “Annealing Induced Evolution of Defect Centers in Epitaxial Silicon Irradiated with High Proton Fluences,” 14th RD50 Workshop, Freiburg (2009).
- [2] L. Makarenko, “Interstitial Defect Reactions in p-type Silicon Irradiated at Different Temperatures,” 15th RD50 Workshop, CERN (2009).
- [3] I. Pintilie, G. Lindström, A. Junkes, and E. Fretwurst, “Radiation-induced Point- and Cluster-related Defects with Strong Impact on Damage Properties of Silicon Detectors,” *Nucl. Instr. and Meth. A* 611, 1, 52 (2009).
- [4] M. Scaringella, “TSC Studies on n- and p-type MCz Si Pad Detectors Irradiated with Neutrons up to 10^{16} n/cm^2 ,” 15th RD50 Workshop, CERN (2009).

- [5] T. Poehlsen, "Charge Collection and Trapping in Epitaxial Silicon Detectors after Neutron Irradiation," 15th RD50 Workshop, CERN (2009).
- [6] J. Lange, "Detailed Investigation of Charge Multiplication Properties in Highly Irradiated Thin Epitaxial Silicon Diodes," 15th RD50 Workshop, CERN (2009).
- [7] V. Eremin, "CCE in Irradiated Silicon Detectors with a Consideration of Avalanche Effect," 15th RD50 Workshop, CERN (2009).
- [8] K. Kaska, "Results on Diodes," 15th RD50 Workshop, CERN (2009).
- [9] A. Srivastava, "Effect of Microscopic Defects in n-type Irradiated MCz Silicon Detectors: Impact on Macroscopic Parameters," 14th RD50 Workshop, Freiburg (2009).
- [10] N. Pacifico, "Annealing of Charge Collection Efficiency in Highly Irradiated MCz-n Strip Detectors," 15th RD50 Workshop, CERN (2009).
- [11] R. Eber, "Mixed Irradiation Studies with Magnetic Czochralski Diodes," 15th RD50 Workshop, CERN (2009).
- [12] G. Kramberger, "Investigation of Electric Field and Charge Multiplication in Irradiated Silicon Detectors by Edge-TCT," 15th RD50 Workshop, CERN (2009).
- [13] A. Affolder, P. Allport, and G. Casse, "Collected Charge of Planar Silicon Detectors after Pion and Proton Irradiations up to 2.2×10^{16} neq cm^{-2} ," Proc. First Int. Conf. on Technology and Instrumentation in Particle Physics, Tsukuba (2009) and accepted by *Nucl. Instr. and Meth. A* [doi:10.1016/j.nima.2010.02.187].
- [14] J. Metcalfe, "Capacitance Measurements and Depletion Voltage for Annealed FZ and MCz Diodes," 14th RD50 Workshop, Freiburg (2009).
- [15] C. Wigglesworth, "Charge Collection Annealing Study of p-in-n Silicon Microstrip Detectors," 15th RD50 Workshop, CERN (2009).
- [16] M. Moll, Ph.D. Thesis, Hamburg University (1999).
- [17] ATLAS TDR 4, CERN/LHCC 97-16 (1997).
- [18] D. Bortoletto, "Simulations of Guard Ring Designs for n-on-p Sensors and of 3D Detectors," 15th RD50 Workshop, CERN (2009).
- [19] M. Schmanau, "New Measurement of Lorentz Angles for Electrons and Holes in Silicon Detectors," 15th RD50 Workshop, CERN (2009).
- [20] Z. Li, "Contributions of Electrons and Holes to Total Collected Charge in Heavily Irradiated Si Pad and Strip/Pixel Detectors: a Comparison Simulation Study," 14th RD50 Workshop, Freiburg (2009).
- [21] A. Zoboli, et al., *IEEE Trans. Nucl. Sci.* 53, 2775 (2008).
- [22] G. Pellegrini, et al., *Nucl. Instr. and Meth. A* 592, 38 (2008).
- [23] G.F. Dalla Betta, et al., "Development of 3D-DDTC Pixel Detectors for the ATLAS Upgrade," paper submitted to *Nucl. Instr. and Meth. A*, arXiv:0910.3629v1.
- [24] G.F. Dalla Betta, et al., "Characterization of 3D-DDTC Detectors on p-type Substrates, *IEEE Nucl. Sci. Symp. Conf. Rec.* N02-4 2009, arXiv:0911.4864v1.
- [25] A. La Rosa, et al., "Preliminary Results of 3D-DDTC Pixel Detectors for the ATLAS Upgrade," PoS(RD09)032, arXiv:0910.3788v1.
- [26] M. Koehler, "Results of Beam Test Measurements with 3D-DDTC Silicon Strip Detectors," 15th RD50 Workshop, CERN (2009).
- [27] M. Gersabeck, "Beam Tests of Medipix2/Timepix Double-sided 3D Detectors," 15th RD50 Workshop, CERN (2009).
- [28] R. Bates, "Charge Collection Studies of Irradiated 3D Detectors," 15th RD50 Workshop, CERN (2009).
- [29] Z. Li, "New Detectors with Novel Electrode Configurations for Applications in sLHC and Photon Sciences," 15th RD50 Workshop, CERN (2009).